Reactive & Functional Polymers 71 (2011) 1119–1128

Contents lists available at SciVerse ScienceDirect

Reactive & Functional Polymers

journal homepage: www.elsevier.com/locate/react

New diphenylamine-based donor–acceptor-type conjugated polymers as potential photonic materials

K.A. Vishnumurthy [a], M.S. Sunitha [a], Reji Philip [b], Airody Vasudeva Adhikari [a,*]

[a] Department of Chemistry, National Institute of Technology Karnataka, Surathkal, Mangalore 575 025, India
[b] Light and Matter Physics Group, Raman Research Institute, C.V. Raman Avenue, Sadashiva Nagar, Bangalore 560 080, India

ARTICLE INFO

Article history:
Received 25 June 2011
Received in revised form 29 August 2011
Accepted 30 August 2011
Available online 10 September 2011

Keywords:
Thiophene
Cyanopyridine
Diphenylamine
Fluorescence

ABSTRACT

A new series of donor–acceptor-type conjugated polymers (**P1** and **P2**) carrying a diphenyl amine moiety were synthesized via Wittig condensation technique. The polymers structures were well established by FT-IR, ^{1}H NMR, elemental analysis and gel permeation chromatographic techniques. They exhibited good thermal stability with an onset decomposition temperature of approximately 325 °C under nitrogen atmosphere. The optical and electrochemical properties of the polymers were studied by UV–vis, fluorescence emission spectroscopy and cyclic voltammetry. They exhibited good fluorescence in dilute solutions and showed solvatochromic behavior in various polar solvents. The electrochemical studies revealed that the polymers possess low-lying LUMO energy levels that ranging from −3.47 to −3.73 eV and high-lying HOMO energy levels that ranging from −5.57 to −5.81 eV. The thirdorder nonlinear optical properties of the polymers were investigated using the Z-scan technique. The effective two-photon absorption (TPA) coefficients (β) of the polymers were found to be 0.645×10^{-10} and 0.212×10^{-10} m/W.

1. Introduction

In recent years, a great deal of interest has been focused on the synthesis of novel π-conjugated polymers because of their intriguing properties, such as electrical conductivity [1], electroluminescence [2], photovoltaic [3] and chemical-sensing [4] properties. Additionally, conjugated polymers have been extensively studied for nonlinear optical (NLO) applications [5–7], such as electro-optical (EO) modulation, optical switches, optical power limiting and frequency doubling, because of their large optical nonlinearity, fast response time, and easy processability for integrated assembly [8–10].

Many conjugated polymeric systems that carry aromatic heterocyclic rings are known to exhibit an increased hyperpolarizability compared to those that carry benzenoid systems [11–13]. This increase in the hyperpolarizability occurs because the delocalization energy of hetero-aromatics is lower than that of benzenoid systems. Active chromophores that contain aromatic heterocycles such as thiophene [14–16], thiazole [17,18] benzothiazole [18,19] or their derivatives are among the most studied systems. Recently, a donor–acceptor (D–A) approach has been adopted to tune the nonlinear properties of conjugated polymers [20]. According to this concept, the incorporation of alternate electron-acceptor and electron-donor units along the main polymer chain would significantly increase the NLO properties, mainly due to an enhancement of the hyperpolarizability. The desired optical properties can be achieved when polymer backbones are tailored with different heterocyclic systems that allow the fine-tuning of important physical and/or photophysical properties.

An extensive literature survey reveals that the incorporation of a 3,4-dialkoxythiophene moiety along the backbone of a polymer enhances the polymer's dopability and decreases its band gap. Furthermore, the incorporation of a highly electron-withdrawing oxadiazole ring along the conjugation path increases the charge-carrying properties of the polymer [21,22], which may alter its NLO properties. In addition, the introduction of vinylene linkages increases the planarity of the polymer chain by reducing the torsional interactions between the hetero-aromatic rings, which leads to a decrease in the band gap [21]. A pyridine ring is also a highly electron-withdrawing moiety that exhibits good electron-transporting abilities and optical properties when it is introduced into the polymer main chain. The presence of a nitrile (CN) substituent on the pyridine ring further enhances the charge-carrying properties of the resulting polymer [23]. Because of the fluorescent nature of cyanopyridine, its presence in a polymer chain would improve the optical properties. Conjugated polymers carrying cyanopyridine are also known to exhibit good optical-limiting properties [24].

In general, the NLO properties of conjugated polymers can be further enhanced either by doping the polymer with a NLO chromophore (guest–host) or covalently incorporating an NLO moiety

* Corresponding author. Tel.: +91 8242474046; fax: +91 8242474033.
E-mail addresses: avadhikari123@yahoo.co.in, avchem@nitk.ac.in (A.V. Adhikari).

1381-5148/$ - see front matter © 2011 Elsevier Ltd. All rights reserved.
doi:10.1016/j.reactfunctpolym.2011.08.011

onto the polymer backbone [22]. The guest–host method has some fatal disadvantages, such as the low solubility of the chromophore in the polymer host, the fast decay of NLO activity due to orientational relaxation and sublimation of the chromophore. However, the method of covalent incorporation of an NLO chromophore leads to an enhancement of the chromophore density without phase separation and is therefore advantageous over the guest–host method. Among the various classes of NLO chromophores reported in the literature, triphenylamine and diphenylamine derivatives are good candidates because of their multifunctional properties, such as good solubility, two-photon absorption, and hole-conducting properties [23,24]. Therefore, the diphenylamine moiety can be conveniently connected with a strong acceptor system through ethylene-conjugated bridges to produce large first-molecular hyperpolarizability in the resulting molecules.

Against this background, we have designed two new D–A type conjugated polymers, **P1** and **P2**, by introducing the highly electron-donating diphenylamine moiety into the polymer network. In the synthetic design of the new polymer **P1**, alkoxythiophene and diphenylamine moieties were connected as electron donors, and an oxadiazole ring was connected as an electron acceptor. In polymer **P2**, a diphenylamine group was attached as the electron donor, and a cyanopyridine ring was used as the electron acceptor. In addition, phenylene vinylene units were incorporated as conjugated spacers in both **P1** and **P2** to enhance the conjugation path length, which in turn enhances their optical properties. In the present work, the required monomers have been prepared from simple thiodiglycolic acid through multistep reactions. The structures of the new **P1** and **P2** polymers have been established by spectral techniques, and their electrochemical, linear and nonlinear optical properties have been evaluated to investigate the influence of their structure on the properties.

2. Experimental

2.1. Materials and methods

3,4-Ditetradecyloxythiophene-2,5-dicarboxylate (structure **8**) was synthesized according to the reported procedure [21]. All chemicals used in the present work were procured from Sigma–Aldrich and Lancaster (UK). All solvents were of analytical grade; they were purchased and used without further purification.

2.2. Instrumentation

Infrared spectra of all intermediate compounds and polymers were recorded on a Nicolet Avatar 5700 FTIR (Thermo). The UV–visible and fluorescence spectra were recorded on a GBC Cintra 101 and a JASCO FP-6200 spectrofluorometer, respectively. ^{1}H NMR spectra were obtained on a Bruker 400 MHz FT-NMR spectrometer using the TMS/solvent signal as an internal reference. Elemental analyses were performed on a Flash EA1112 CHNS analyzer (Thermo Electron Corporation). Mass spectra were recorded on a Jeol SX-102 (FAB) mass spectrometer. Electrochemical studies were performed using an AUTOLAB PGSTAT30 electrochemical analyzer. Molecular weights of the polymers were determined with a gel permeation chromatograph (GPC) against polystyrene standards with THF as the eluent.

2.3. Synthetic plan

Schemes 1 and 2 show the synthetic routes for the preparation of new monomers and their polymerization to the target polymers. In Scheme 1, compound **1** was alkylated using tetradecyl bromide in the presence of sodium hydride to produce alkylated diphenylamine **2**, which was later converted into the corresponding dialdehyde **3** via the Vilsmeyer–Haak reaction. In Scheme 2, the required chalcone **4** was prepared from tolualdehyde and 4-methylacetophenone using the Claisen–Schmidt reaction. The product was then cyclized to cyanopyridine **5** by reaction with malononitrile in the presence of sodium methoxide. Further, two methyl groups of compound **5** were brominated via the Wholzigler method using NBS and BPO. The resulting dibromo derivative **6** was conveniently converted to phosphonium Wittig salt **7**, which, upon treatment with dicarboxaldehyde **3** in ethanol–chloroform medium, yielded polymer **P2** in good yield.

As shown in Scheme 2, the diesters of 3,4-ditetradecyloxy thiophene were readily converted to 3,4-ditetradecyloxythiophene-2,5-carboxydihydrazides **9** by the action of hydrazine hydrate in alcoholic medium. This dihydrazide was tolylated to yield 3,4-bis(tetradecyloxy)-N′2,N′5-bis(4-methylbenzoyl)thiophene-2,5-dicarbohydrazide **10**, which, upon treatment with phosphorus oxychloride gave 5,5′-(3,4-bis(tetradecyloxy) thiophene-2,5-diyl)bis(2-p-tolyl-1,3,4-oxadiazole) **11** [25] in good yield. This bisoxadiazole compound **11** was then Wohl–Ziegler brominated using N-bromo succinimide (NBS) in carbon tetrachloride, and the resulting 5,5′-(3,4-bis(tetradecyloxy)thiophene-2,5-diyl)bis(2-(4-(bromomethyl)phenyl)-1,3,4-oxadiazole) **12** was further converted to 5,5′-(3,4-bis(tetradecyloxy)thiophene-2,5-diyl)bis(2-(4-triphenylphosphonionmethyl)phenyl)-1,3 ,4 oxadiazole) **13** upon treatment with triphenylphosphine in the presence of DMF. The reaction of compound **13** with diphenylaminedicarboxaldehyde **3** in ethanol–chloroform medium yielded polymer **P1**.

2.4. Syntheses of intermediates, monomers and polymers

2.4.1. Synthesis of N-tetradecyl diphenylamine *2*

Sodium hydride (0.7185 g, 29.5 mmol) was added to the solution of diphenylamine **1** (5 g, 29.5 mmol dissolved in 50 ml of DMF) and the resulting mixture was stirred for approximately 30 min. 1-Bromo tetradecane (8.29 g, 29.5 mmol) was then slowly added to the reaction mixture, and the mixture was stirred for 5 h at room temperature. After completion of the reaction, the resulting mixture was extracted with ethyl acetate/brine and then dried with Na_2SO_4. The solvent was removed by evaporation. The resulting crude product was purified by column chromatography using hexane and ethyl acetate. Yield: 8.8 g (82%). ^{1}H NMR (400 MHz, $CDCl_3$), δ (ppm): 7.36–7.04 (m, 10H, aromatic protons), 3.83 (t, 2H, —NCH_2), 1.74 (m, 2H, —NCH_2CH_2—), 1.34–1.24 (m, 24H, —CH_2CH_2), 0.87 (t, 3H, CH_3). FTIR (cm^{-1}): 2920, 2852, 1590, 1494, 1309, 891, 743. Anal. Calcd for $C_{26}H_{39}N$: C, 85.42; H, 10.75; N, 3.83. Found: C, 85.45; H, 10.78; N, 3.84.

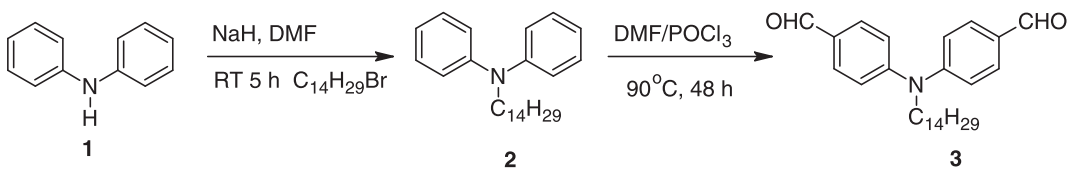

Scheme 1. Synthesis of N-substituted diphenylamine dialdehyde.

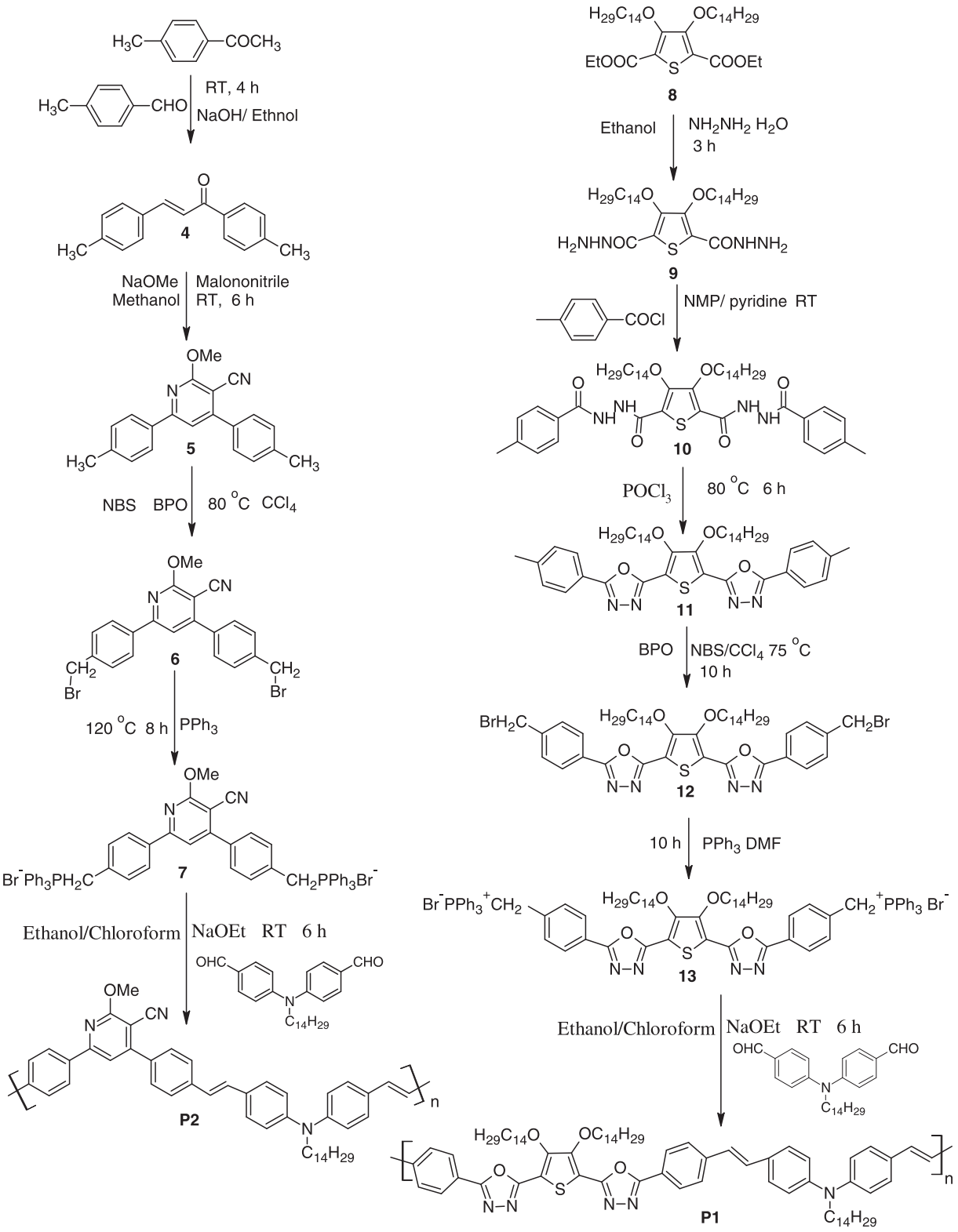

Scheme 2. Synthesis scheme for monomers and polymers.

*2.4.2. Synthesis of N-tetradecyl-diphenylamine-4,4′-dicarbaldehyde **3***

Freshly distilled phosphorous oxychloride (12.6 ml, 82.6 mmol) was added drop-wise to 5.5 ml of anhydrous DMF at 0 °C over a period of 30 min. Later, alkylated diphenylamine **2** (5 g, 13.6 mmol in 20 ml of 1,2-dichloroethane) was added to the above solution and stirred at 90 °C for 48 h. This solution was cooled to room temperature, poured into ice water, and neutralized to pH 6–7 by the drop-wise addition of saturated sodium hydroxide solution. The dialdehyde **3** was extracted with ethyl acetate. The organic layer was dried with anhydrous Na_2SO_4, and the solvent was subsequently removed under reduced pressure. The crude product was purified by column chromatography. A light-orange solid

was obtained. Yield: 4.1 g (71%). ^{1}H NMR (400 MHz, CDCl3), δ (ppm): 9.88 (s, 2H, aldehydic), 7.81 (d, 4H, aromatic), 7.14 (d, 4H, aromatic protons), 3.83 (t, 2H, NCH_2), 1.74 (m, 2H, —NCH_2CH_2—), 1.34–1.24 (m, 24H, —CH_2CH_2), 0.87 (t, 3H, CH_3). FTIR (cm^{-1}): 2915, 2848, 1685, 1578, 1502, 1359, 1157, 820, 719. Element. Anal. Calcd. for $C_{28}H_{39}NO_2$: C, 79.76; H, 9.32; N, 3.32. Found: C, 76.79; H, 9.28; N, 3.35 (Scheme 1).

2.4.3. Synthesis of 1,3-bis(4-methylphenyl)prop-2-en-1-one ***4***

A mixture of p-tolualdehyde (5 g, 41.6 mmol) and 4-methylacetophenone (5.5 g, 41.6 mmol) was dissolved in 50 ml of ethanol and stirred in the presence of potassium hydroxide solution (2.3 g in 5 ml water) at room temperature. After 10 h, the obtained solid was filtered; it was recrystallized from a chloroform–methanol system to produce a yellow needle-shaped solid. Yield: 8.9 g (90%). FTIR (cm^{-1}): 1644, 1591, 1169, 987, 805, 726. Element. Anal. Calcd. for $C_{17}H_{16}O$: C, 86.40; H, 6.82. Found: C, 86.41; H, 6.84.

2.4.4. Synthesis of 2-methoxy-4,6-bis(4-methylphenyl)pyridine-3-carbonitrile ***5***

Compound **4** (5 g, 21.1 mmol) was added slowly to a freshly prepared sodium alkoxide solution (223.3 mmol of sodium in 100 ml of methanol) with stirring. Malononitrile (1.39 g, 21.1 mmol) was then added with continuous stirring at room temperature until the reaction was complete. The separated solid was collected by filtration and recrystallized from hot ethanol and chloroform. Yield: 4.5 g (67%). M.p.: 142–144 °C. ^{1}H NMR (400 MHz, $CDCl_3$) δ (ppm): 8.00 (m, 2H, Ar—H), 7.55 (m, 2H, Ar—H), 7.44 (s, 1H, Ar—H (pyridine)), 7.34–7.28 (m, 4H, Ar—H), 4.19 (s, 3H, —O—CH_3), 2.43 (s, 6H, Ar—CH_3). FTIR (cm^{-1}): 2907, 2217, 1658, 1554, 1366, 1139, 818. Element. Anal. Calcd. for $C_{21}H_{18}N_2O$: C, 80.23; H, 5.77; N, 8.91. Found: C, 80.25; H, 5.75; N, 8.93.

2.4.5. Synthesis of 4,6-bis[4-(bromomethyl)phenyl]-2-methoxypyridine-3-carbonitrile ***6***

A mixture of compound **5** (3 g, 9.5 mmol), N-bromosuccinimide (1.38 g, 19.1 mmol), and 5 mg of benzoyl peroxide in 30 ml of carbon tetrachloride was refluxed for 8 h. After the solvent was removed, 20 ml of water was added with stirring for 1 h. The resulting crude product was recrystallized from an ethyl acetate/chloroform mixture to produce pure white-colored solid. Yield: 3.5 g (77%). M.p.: 202–205 °C. ^{1}H NMR (400 MHz, $CDCl_3$) δ (ppm): 8.00 (m, 2H, Ar—H), 7.99–7.55 (m, 4H, Ar—H), 7.5–7.3 (m, 2H, Ar—H), 7.29 (s, 1H, Ar—H (pyridine)), 4.81 (s, 6H, Ar—CH_3), 4.13 (3H, —O—CH_3). FTIR (cm^{-1}): 2993, 2219, 1580, 1546, 1359, 1139, 1007, 821, 600. Element. Anal. Calcd. for $C_{21}H_{16}Br_2N_2O$: C, 53.42; H, 3.42; N, 5.93. Found: C, 53.46; H, 3.45; N, 5.94.

2.4.6. Synthesis of [4,6-bis[44-triphenyl phosphonion methyl) phenyl]-2-methoxy, 3-cyano pyridine]dibromide ***7***

A solution of dibromide compound **6** (1 g, 6.3 mmol) and triphenyl phosphine (3.34 g, 12.7 mmol) in 5 ml of DMF was refluxed with stirring for 8 h. The reaction mixture was cooled to room temperature and poured into 50 ml of ethyl acetate. The resulting mixture was sonicated for approximately 30 min to induce precipitation. The obtained white-colored amorphous solid was filtered off, washed with an excess of ethyl acetate and dried at 40 °C for 10 h. Yield: 82%. M.p.: above 300 °C. ^{1}H NMR (400 MHz, $CDCl_3$) δ (ppm): 8.14–8.12 (m, 2H, Ar—H), 7.99–7.50 (m, 33H, Ar—H), 7.16–7.12 (m, 4H, Ar—H), 5.26 (s, 4H, Ar—CH_2), 4.13 (s, 3H, —O—CH_3). FTIR (cm^{-1}): 3365, 3051, 2853, 2211, 1658, 1430, 1103, 728, 682, 495. Element. Anal. Calcd. for $C_{57}H_{46}Br_2N_2OP_2$: C, 68.68; H, 4.65; N, 2.81. Found: C, 68.66; H, 4.68; N, 2.84.

2.4.7. Synthesis of 3,4-ditetradecyloxythiophene-2,5-carboxydihydrazide ***9***

Diethyl-3,4-dialkoxythiophene-2,5-dicarboxylate (0.5 g) was added to a solution of 5 ml of hydrazine monohydrate in 40 ml of ethanol. The reaction mixture was refluxed for 3 h. After the solution was cooled to room temperature, a white precipitate was obtained. The precipitate was filtered, washed with petroleum ether, dried under vacuum and finally recrystallized from ethanol to produce a white crystalline solid. Yield: 92%. FTIR (cm^{-1}): 3412 (—NH_2), 3341 (—NH—), 2915, 2848, 1650 (>C=O), 1501, 1302, 1043, 956, 720.

2.4.8. Synthesis of N2,N5-di-(4-methylbenzoyl)-3,4-ditetradecyloxy thiophene-2,5-dicarbo hydrazide ***10***

To a clear mixture of dihydrazide **9** (5 g, 8.79 mmol) and 2 ml of pyridine in 50 ml of NMP, two equivalents (2.71 g, 17.58 mmol) of 4-methylbenzoyl chloride was added slowly at room temperature while stirring. The stirring was continued at room temperature for 1 h. The resulting solution was stirred at 80 °C for 5 h. After cooling to room temperature, the reaction mixture was poured into an excess of water to produce a precipitate. The precipitate was collected by filtration, washed with an excess of water, dried in oven and recrystallized from an ethanol/chloroform mixture to produce the desired product. Yield: 82%. ^{1}H NMR (400 MHz, $CDCl_3$), δ (ppm): 10.22 (s, 2H, —NH—), 9.71 (s, 2H, —NH—), 7.75 (d, 4H, Ar, J = 8.4 Hz), 7.15 (d, 4H, Ar, J = 8.0 Hz), 4.24 (t, 4H, —OCH_2—, J = 7.0 Hz), 2.38 (s, 6H, Ar—CH_3), 1.12–1.84 (m, 40H, —$(CH_2)_{12}$—) 0.80 (t, 6H, —CH_2—CH_3, J = 7.4 Hz). FTIR (cm^{-1}): 3245 (—CO—NH—), 2917, 2849 (aromatic), 1666, 1621, 1447, 1274, 1046, 835, 732. Element. Anal. Calcd. for $C_{50}H_{76}N_4O_6S$: C, 69.73; H, 8.89; N, 6.51; S, 3.72. Found: C, 69.72; H, 8.84; N, 6.53; S, 3.71.

2.4.9. Synthesis of 2,2′-(3,4-ditetradecyloxythiophene-2,5-diyl)bis[5-(4-methylphenyl)-1,3,4-oxadiazole] ***11***

A mixture of compound **10** (5 g, 6.2 mmol) and 50 ml of phosphorus oxychloride was stirred at 80 °C for 6 h. The reaction mixture was then cooled to room temperature and poured into an excess of ice-cold water. The resulting precipitate was collected by filtration, washed with water and dried in an oven. Further purification was performed by recrystallization of the obtained solid from an ethanol/chloroform mixture. Yield: 85%. M.p.: 98–100 °C. ^{1}H NMR (400 MHz, $CDCl_3$) δ (ppm): 7.94 (d, 4H, Ar, J = 8.4 Hz), 7.29 (d, 4H, Ar, J = 8.0 Hz), 4.25 (t, 4H, —O—CH_2—, J = 6.6 Hz), 2.38 (s, 6H, Ar—CH_3), 1.13–1.83 (m, 48H, —$(CH_2)_{12}$—), 0.82 (t, 6H, —CH_2—CH_3, J = 7.0 Hz). FTIR (cm^{-1}): 2915, 2848, 1587 (—C=N—), 1556, 1481, 1465′, 1279, 1054, 823, 726. Element. Anal. Calcd. for $C_{50}H_{72}N_4O_4S$: C, 72.77; H, 8.79; N, 6.79; S, 3.89. Found: C, 72.72; H, 8.72; N, 6.81; S, 3.9.

2.4.10. Synthesis of 2,20-(3,4-ditetradecyloxythiophene-2,5-diyl)bis[5-(4-bromomethylphenyl)-1,3,4-oxadiazole] ***12***

A mixture of compound **12** (3 g, 3.9 mmol), N-bromosuccinimide (1.38 g, 7.8 mmol) and 5 mg of benzoyl peroxide in 30 ml of benzene was refluxed for 5 h. After the solvent was removed, 20 ml of water was added with stirring for 1 h. The resulting crude product was recrystallized from a methyl acetate/chloroform mixture. Yield: 65%. ^{1}H NMR (400 MHz, $CDCl_3$) δ (ppm): 7.92 (d, 4H, Ar, J = 8.4 Hz), 7.27 (d, 4H, Ar, J = 8.0 Hz), 4.5 (s, 4H, Ar—CH_2—Br), 4.24 (t, 4H, —O—CH_2—, J = 6.6 Hz), 1.13–1.83 (m, 40H, —$(CH_2)_{12}$—), 0.80 (t, 6H, —CH_2—CH_3, J = 7.0 Hz). FTIR (cm^{-1}): 2915, 2849, 1557 (—C=N—), 1482, 1465, 1279, 1054, 952, 822, 726. Element. Anal. Calcd. for $C_{50}H_{70}Br_2N_4O_4S$: C, 61.09; H, 7.18; N, 5.70; S, 3.26. Found: C, 61.05; H, 7.15; N, 5.71; S, 3.28.

*2.4.11. Synthesis of 2,20-(3,4-ditetradecyloxythiophene-2,5-diyl)bis[5-((4-triphenyl phosphonium methyl)phenyl)-1,3,4-oxadiazole] dibromide **13***

A solution of dibromide compound **12b** (1 g, 1.07 mmol) and triphenyl phosphine (0.565 g, 2.157 mmol) in 5 ml of DMF was refluxed with stirring for 10 h. The reaction mixture was cooled to room temperature and poured into 50 ml of ethyl acetate. The resulting precipitate was collected by filtration, washed with an excess of ethyl acetate and dried at 40 °C for 10 h. (**13b**) Yield: 72%. M.p.: above 300 °C. ^{1}H NMR (400 MHz, $CDCl_3$), δ (ppm): 7.21–7.90 (m, 38H, Ar—H), 5.95 (s, 4H, Ar—CH_2—P—), 4.25 (t, 4H, —OCH_2—, J = 6.9 Hz), 1.12–1.83 (m, 48H, —$(CH_2)_{12}$—), 0.79 (t, 6H, —CH_2—CH_3, J = 7.0 Hz). FTIR (cm^{-1}): 2922, 2855, 1583, 1459, 1352, 1048, 956, 727. Element. Anal. Calcd. for $C_{86}H_{100}Br_2N_4O_4P_2S$: C, 68.52; H, 6.69; N, 3.72; S, 2.13. Found: C, 68.58; H, 6.66; N, 3.38; S, 2.23.

*2.4.12. General procedure for the synthesis of polymers **P1** and **P2***

Monomer **3** (0.5 g, 0.11 mmol) and monomer **13** (1.7 g, 0.11 mmol) were dissolved in a mixture of 5 ml of chloroform and 15 ml of ethanol. Sodium ethoxide (0.020 g, 1 mmol in 10 ml of ethanol) was added to the reaction mass at room temperature under a nitrogen atmosphere. Then the reaction mixture turned yellow in color. It was stirred for 12 h at room temperature. After the completion of the reaction, solvent was removed under reduced pressure. The crude reaction mass was then poured into an excess of methanol and stirred for approximately 30 min. The obtained polymer was filtered and then washed thoroughly with acetone, re-dissolved in chloroform and poured into excess of methanol to remove the oligomers. The resulting precipitate was collected by filtration and dried under vacuum for 24 h to give a greenish-yellow-colored powder. Polymer **P2** was prepared by a similar method (Scheme 2). The characterization data of **P1**and **P2** are given below.

P1: ^{1}H NMR, (400 MHz, CDCl3), δ (ppm): 8.1–7.1 (m, 12H, Ar—H), 7.1–6.9 (m, 2H, —CH=CH—), 4.31 (m, 4H, —O—CH_2—), 3.73–3.71 (m, 2H, —NCH_2—), 2.2–1.1 (m, 72H, aliphatic), 0.87 (t, 9H, —CH_2CH_3). FTIR (cm^{-1}): 2919, 2850, 1585, 1499, 1366, 1175, 827, 726. Weight-average molecular weight (M_w): 12,900.

P2: ^{1}H NMR, (400 MHz, CDCl3), δ (ppm): 8.2–7.0 (m, 16H, Ar—H), 7.0–6.8 (m, 2H, —CH=CH—), 4.20 (m, 4H, —O—CH_3), 3.72–3.69 (m, 2H, —NCH_2—), 2.2–1.1 (m, 24H, aliphatic), 0.87 (t, 3H, —CH_2CH_3). FTIR (cm^{-1}): 2919, 2849, 2217, 1579, 1503, 1356, 1237, 1009, 818. Weight-average molecular weight (M_w): 8400.

3. Results and discussion

3.1. Characterization

The structures of the intermediates and the target polymers were established by elemental analysis and spectroscopic techniques. The structure of the dicarboxaldehyde monomer **3** was confirmed by ^{1}H NMR and FTIR spectroscopic measurements. The ^{1}H NMR spectra of the monomer **3** showed peaks at δ 9.88 that correspond to aldehydic protons, and its FTIR spectrum showed a strong peak at 1685 cm^{-1}, which confirms the presence of aldehydic protons. The spectral characteristics of chalcone **4** matched the reported data. The cyclization of the chalcone to cyanopyridine **5** was confirmed by the ^{1}H NMR spectrum of **5**, which showed a signal at δ 4.19 that corresponds to —OCH_3 protons of the pyridine ring. The FTIR spectrum of **5** displayed a sharp peak at 2217 cm^{-1}, which indicates the presence of cyano groups. The formation of compound **6** was confirmed by its ^{1}H NMR spectrum, in which it showed a signal at δ 4.81 that corresponds to tolyl methyl protons. These protons are deshielded to a greater extent than those in compound **5**. The structure of monomer **7** was also evidenced by its ^{1}H NMR data; the methyl protons of its phosphonium salt resonated at δ 5.26 and were substantially deshielded compared to those of compound **6**.

Similarly, the structure of 3,4-ditetradecyloxythiophene-2,5-carboxydihydrazide (**9**) was established by its FTIR and ^{1}H NMR spectra. Its FTIR spectrum showed sharp peaks at 3412 and 1650 cm^{-1}, which indicate the presence of —NH_2 and >C=O groups, respectively. Its ^{1}H NMR spectrum displayed sharp singlets at δ 8.3 and δ 4.9 for the —NH— and —NH_2 protons, respectively. The conversion of bishydrazide **9** to biscarbohydrazide **10** was confirmed by the FTIR and elemental analysis studies. The biscarbohydrazide exhibited sharp peaks at 3245 and 1666 cm^{-1}, which indicate the presence of —NH— and >C=O groups, respectively. Furthermore, its ^{1}H NMR spectrum showed peaks at δ 2.38, δ 10.22 and δ 9.71, which indicate the presence of the tolyl methyl protons and amidic protons, respectively. The formation of compound **10** from **11** was established by FTIR, ^{1}H NMR and mass spectral analyses. The disappearance of bands in the regions at 3245 and 1666 cm^{-1} and the appearance of a new band at 1587 cm^{-1} indicate the formation of an oxadiazole ring in the molecule. The formation of the ring was further confirmed by the ^{1}H NMR spectrum, which showed no characteristic peaks due to amidic protons and deshielding of the aromatic protons. The conversion of compound **11** to compound **12** was confirmed by ^{1}H NMR studies and elemental analysis. In the ^{1}H NMR spectrum of **12**, the disappearance of the tolyl methyl protons and the appearance of a new peak at δ 4.5 confirms the bromination of the methyl groups attached to the aromatic rings. The formation of compound **13** was further confirmed by ^{1}H NMR studies and elemental analysis. The ^{1}H NMR spectrum showed a peak at δ 5.95, which indicates the presence of a —CH_2— group attached to the aromatic ring and a phosphonium group on either side. The structures of both polymers were established by ^{1}H NMR, FTIR and gel permeation chromatographic techniques.

The weight-average molecular weights of the polymers **P1** and **P2** were 12,900 and 8400, respectively. The polydispersity of these polymers were 2.2 and 1.90, respectively. The thermal stability of these polymers was studied by thermogravimetric analysis (TGA) in a nitrogen atmosphere using a 3 °C min^{-1} temperature ramp from 50 to 700 °C. The thermogram (Fig. 1) showed that the polymers exhibit a high thermal stability. The loss of less than 6–8% weight at temperatures less than 300 °C may be attributed to the degradation of the alkyl and alkoxy side chains in the polymers. The gradual weight loss above 300 °C may be attributed to the degradation of the polymer backbone, which led to the residue. Similar

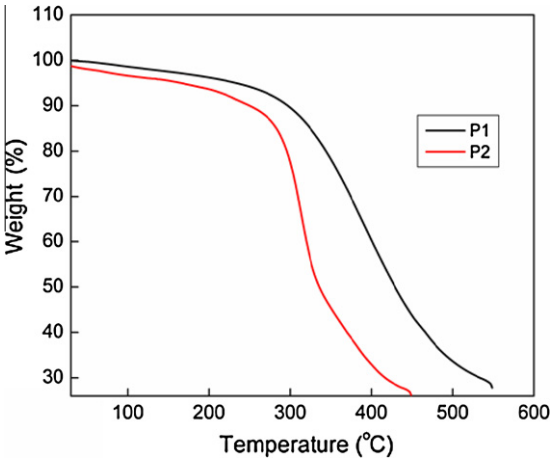

Fig. 1. Thermogravimetric traces of **P1** and **P2.**

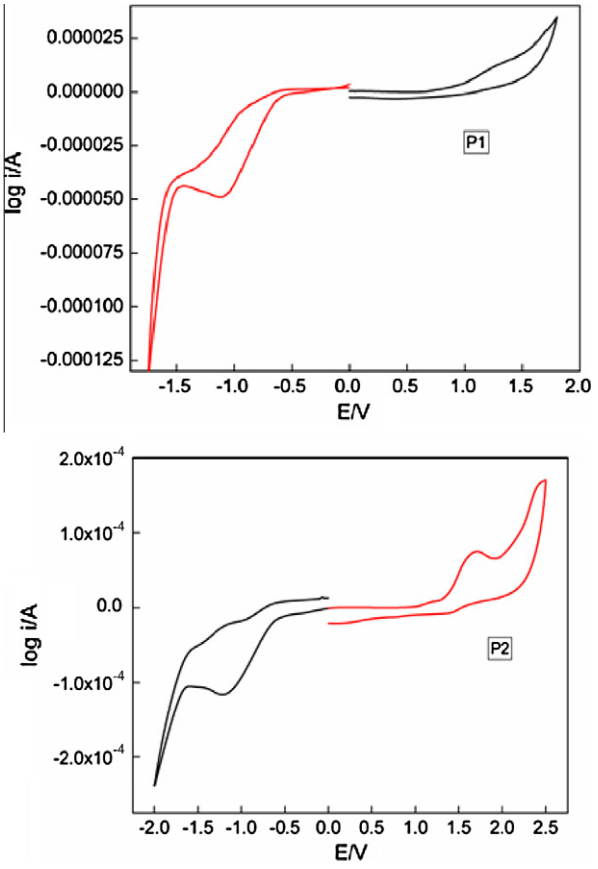

Fig. 2. Cyclic voltammetric traces of **P1** and **P2**.

behavior has been observed for some of the reported polythiophenes [26,27]. The newly synthesized polymer is soluble in common organic solvents such as chloroform, dichloromethane, tetrahydrofuran and dimethylsulfoxide, and this polymer showed good processability and film-forming ability. The solubility may be attributed to the presence of bulky alkyl and alkoxy groups on the aromatic rings in the polymers.

3.2. Electrochemical studies

Cyclic voltammetry (CV) was employed to determine redox potentials of the new polymers and to estimate the HOMO and LUMO levels, which is important in determining the band gap. Cyclic voltammograms of the polymers coated on a glassy carbon electrode were obtained on an AUTOLAB PGSTAT-30 electrochemical analyzer using a Pt counter electrode and an Ag/AgCl reference electrode immersed in an electrolyte [0.1 M $(n\text{-}Bu)_4NClO_4$ in acetonitrile] at a scan rate of 25 mV/s [28].

All the measurements were calibrated using ferrocene as a standard [29]. As shown in Fig. 2, the newly synthesized polymers were electroactive either in the cathodic region or in the anodic region. The onset oxidation potentials (p-doping) were estimated to be 1.09 and 1.41 eV for **P1** and **P2**, respectively. For the n-doping (reduction) process, the onset reduction potentials for the polymers appeared at −0.93 and −0.67 eV for **P1** and **P2**, respectively. These reduction potentials are even lower than that of 2-(4-biphenylyl)-5-(4-*tert*-butylphenyl)-1,3,4-oxadiazole, PBD) the most widely used electron-transporting material in polymer light emitting diodes PLEDs. The onset oxidation and reduction potentials were used to estimate the highest occupied molecular orbital (HOMO) and lowest unoccupied molecular orbital (LUMO) energy levels of the polymers. The equations, $E_{HOMO} = -\left[E^{oxd}_{onset} + 4.4\ eV\right]$ and $E_{LUMO} = -\left[E^{red}_{onset} - 4.4\ eV\right]$, where E^{oxd}_{onset} and E^{red}_{oxd} are the onset potentials vs. a standard calomel electrode (SCE) for the oxidation and reduction of the referred material, were used for the calculation. The electrochemical potentials and energy levels of the polymer are tabulated in Table 1. The HOMO energy levels of polymers **P1** and **P2** are estimated to be 5.57 and 5.81 eV, respectively. These values are almost the same as that of poly(cyanoterphthalylidene) (CNPPV), which indicates that the polymers have a hole-injection ability similar to that of CNPPV when they are used in PLEDs. The LUMO energy levels of polymers **P1** and **P3** are estimated to be 3.47 and 3.73 eV, respectively. These values are greater than those of CN-PPV (3.02 eV), which indicates that these polymers exhibit better electron-injection ability when they are used in PLEDs [21,30]. The electrochemical band gaps of the polymers were calculated from the difference between HOMO and LUMO energy levels and were 2.1 and 2.0 eV for polymers **P1** and **P2**, respectively.

The electrochemical behavior of these polymers can be explained on the basis of their structure–activity relationship. In general, when electron-withdrawing substituents are attached to conjugated molecules, the electron density in the π-system of the conjugated molecule will be decreased. Consequently, the molecule will be stabilized and its oxidation potential will be increased. This results in a shift of the HOMO energy level to a lower energy. Similarly, the presence of tetradecyloxythiophene and N-tetradecyldiphenylamine units in **P1** and **P2** influences the HOMO energy level because of their strong electron-donating ability. Usually, the band gap of any conjugated polymer can be influenced by conjugation length, solid-state intermolecular ordering and the presence of electron-withdrawing or electron-donating moieties. The variation of these properties allows the optical and electrochemical behavior of such polymers to be tuned. The effective conjugation length, which is dependent upon the torsional angle between the repeating units along the polymer backbone, can be controlled by the introduction of sterically hindered bulky alkoxy side chains to twist the units out of plane [31]. In this context, diphenylamine-carrying bulky alkyl substituents have a major role in the enhancement of oxidation potentials [32].

3.3. Linear optical properties

The solution-phase UV–vis absorption and fluorescence emission spectra of the new polymers were recorded at room temperature in dilute solutions. All spectral data are summarized in Table 2. UV–vis absorption spectra were recorded in different polar solvents (Figs. 3 and 4). The enhancement in the absorption maximum of polymer **P2** is attributed to the strong electron-withdrawing nature of the cyanopyridine along the polymer backbone. The absorption maximum of polymer **P1** was blue-shifted compared to that of **P2**. This shift is most probably due to the pres-

Table 1
Electrochemical characterization table.

Polymer	E_{oxd}	E_{red}	E_{oxd} (onset)	E_{red} (onset)	E_{HOMO} (eV)	E_{LUMO} (eV)	E_g (eV)
P1	1.17	−1.46	1.09	−0.93	−5.57	−3.47	2.1
P2	1.69	−1.20	1.41	−0.67	−5.81	−3.73	2.0

Table 2
UV absorption and fluorescence emission spectra of **P1** and **P2** in different polar solvents.

Polymers	UV–visible absorption and fluorescence emissions in different solvents (nm) [(UV–visible) fluorescence emission]				Quantum yield
	Chlorobenzene	Chloroform	Tetrahydrofuran	Dimethyl sulfoxide	In THF (%)
P1	(443) 525	(446) 532	(458) 536	(460) 547	39
P2	(458) 540	(465) 548	(472) 555	(484) 570	44

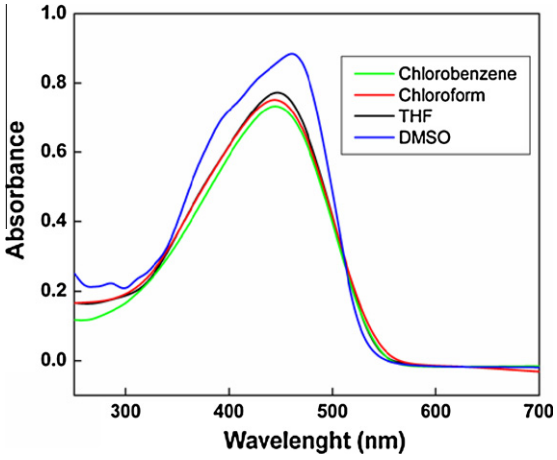

Fig. 3. UV absorption spectra of **P1** in different polar solvents.

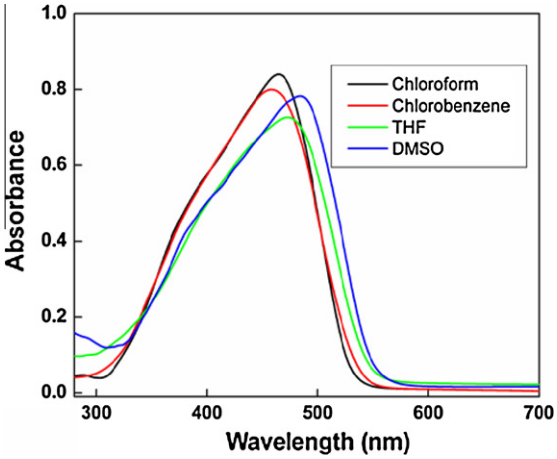

Fig. 4. UV absorption spectra of **P2** in different polar solvents.

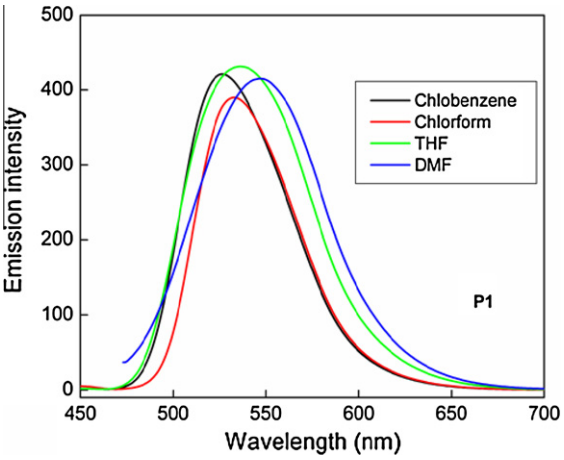

Fig. 5. Fluorescence emission spectra of **P1** in different polar solvents.

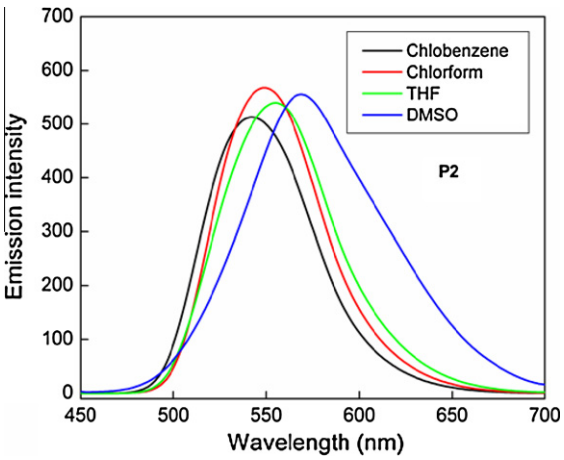

Fig. 6. Fluorescence emission spectra of **P2** in different polar solvents.

ence of the alkoxy groups on the thiophene ring of the polymer backbone, which usually leads to an increase in the dihedral angle of consecutive aromatic units. The increased dihedral angle results in the reduction of the electronic conjugation and hence induces an enhanced band gap [33].

Fluorescence studies of **P1** and **P2** were performed in different polar solvents (Figs. 5 and 6). The polymers displayed very good fluorescence behavior in different solvents when irradiated with UV light (Figs. 7 and 8). The fluorescence emission spectra were obtained by irradiative excitation at the wavelength of the absorption maximum. The polymers exhibited a strong solvatochromic effect [34,35]. Based on the results of these studies, the emission maxima of the polymers were red-shifted as the polarity of the solvent was increased. In particular, maximum solvatochromism was observed in **P2** because of the presence of the cyanopyridine ring in the backbone. In a highly polar solvent such as THF or DMSO, the emissive S_1 state of the intra-molecular charge transfer (ICT) is strongly solvated, and its energy is therefore dramatically decreased. Consequently, the energy gap $E(S_1, S_2)$ is enlarged so that the coupling of the S_1 state directly to the ground state stays open, and the inter-system crossing from the S_1 to the T state is enhanced [36,37].

The presence of high-electron-releasing thiophene and diphenyl amine moieties along the polymer chain was observed to induce a red shift (lower energy) of their emission maxima. This shift is mainly attributed to energy losses through dissipation of vibrational energy during the decay. This is normally influenced by interaction between the fluorophore and the solvent molecules around the excited dipole, by hydrogen bonding and by the formation of charged complexes. In addition, the introduction of the pyridinyl moiety in polymer **P2** increases its electron affinity, which makes the polymer more resistant to oxidation and also gives the polymer better electron-transporting properties. Furthermore, it avoids fluorescence quenching due to the inter-system crossing (ISC) effect [38]. The quantum yield for emission in solu-

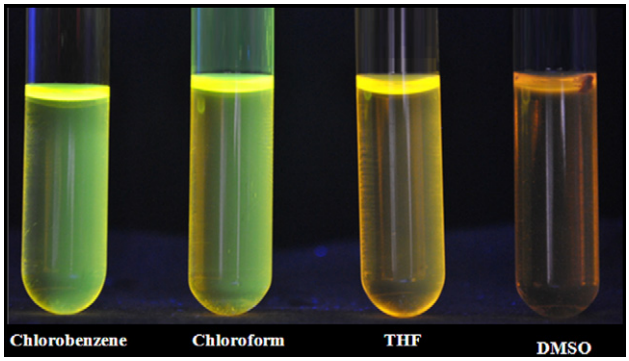

Fig. 7. Fluorescence emission of **P1** in different polar solvents under UV irradiation.

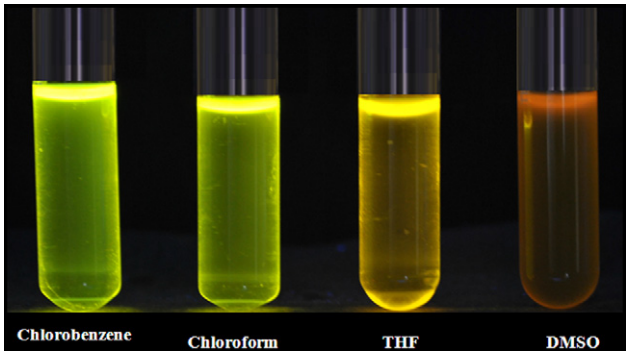

Fig. 8. Fluorescence emission of **P2** in different polar solvents under UV irradiation.

tion was determined relative to quinine sulfate in 0.1 M H_2SO_4 according to the method described by John et al. [39] and Davey et al. [40]. Polymers **P1** and **P2** were strongly emissive with high quantum yields. These high quantum yields could be attributable to the rigid structure of the polymer with the effect that relaxation from the excited state through non-radiative (e.g., thermal) processes would be reduced with consequently higher fluorescence quantum yields [41].

3.4. Third-order nonlinear optical activity

3.4.1. Z-scan studies

A very convenient and fast experimental method to assess materials for NLO (including optical limiting) is the Z-scan experiment [42]. This method allows the measurement of the magnitude of both the nonlinear refraction (NLR) and nonlinear absorption (NLA) as a function of the incident laser intensity while the sample is gradually moved through the focus of a lens (along the *z*-axis). In the experiment, the sample is placed in the path of a high-intensity laser beam at different positions with respect to the focus (different values of *z*), and the corresponding transmission is measured. The sample is then exposed to different laser intensity at each position; therefore, its position-dependent transmission will give information on its intensity-dependent transmission as well. The effective nonlinear absorption coefficients were calculated by fitting theory. We used a stepper-motor-controlled linear translation stage in our setup to move the sample through the beam in precise steps. The sample was placed in a 1-mm cuvette. The transmission of the sample at each point was measured using two pyroelectric energy probes (Rj7620, Laser Probe, Utica, NY, USA). One energy probe monitored the input energy while the other monitored the energy transmitted through the sample. The second harmonic output (532 nm) of a Q-switched Nd:YAG laser (Quanta Ray, Spectra Physics) was used to excite the molecules. The temporal width (FWHM) of the laser pulses was 7 ns. The pulses were fired in the "single shot" mode, which allowed sufficient time between successive pulses to avoid accumulative thermal effects in the sample.

Fig. 9 shows the open-aperture Z-scan curves of the polymers in THF solutions. In each case, we observed two-photon absorption (TPA). The nonlinear activity of the polymer can be explained by considering pulse duration, pump intensity and wavelength. It can be explained by the transitions: ground state S_0 to higher excited singlet states S_n (two-photon or multi-photon excitation), the first excited singlet state S_1 to higher excited states S_n, or the T_1 to T_n states in the triplet manifold. The last two processes are known as excited-state absorption (ESA), and if their cross-sections are larger than that of the ground-state linear absorption, then these processes are referred to as reverse saturable absorption (RSA). The net effect is then known as an "effective" TPA process.

The nonlinear transmission behavior of the present samples can therefore be modeled by defining an effective nonlinear absorption coefficient $\alpha(I)$, as given by:

$$\alpha(I) = \frac{\alpha_0}{1 + \left(\frac{I}{I_s}\right)} + \beta I \tag{1}$$

where α_0 is the unsaturated linear absorption coefficient at the wavelength of excitation, I_s is the saturation intensity (intensity at which the linear absorption drops to half its original value), and β is the effective TPA coefficient. To calculate the output laser intensity for a given input intensity, we first numerically evaluated the output intensity from the sample for each input intensity by solving the propagation:

$$\frac{dI}{dz'} = -\left[\left(\alpha_0 / \left(1 + \frac{I}{I_s}\right)\right) + \beta I\right] I \tag{2}$$

using the fourth-order Runge–Kutta method. The input intensities for the Gaussian laser beam for each sample position in the Z-scan are calculated from the input energy, laser pulse width and irradiation area. Here, 'Z' indicates the propagation distance within the sample. The normalized transmittance was then calculated by dividing the output intensity by the input intensity and normalizing it with the linear transmittance. As seen from Fig. 8, there is good agreement between the experimental data and the numerical simulation. The numerically estimated values of the effective TPA coefficients are 0.64×10^{-10} and 0.21×10^{-10} m/W for polymers **P1** and **P2**, respectively.

For comparison, under similar excitation conditions, good NLO materials like copper (Cu) nanocomposite glasses have shown effective TPA coefficient values of 10^{-10}–10^{-12} m/W [43], functionalized carbon nanotubes have shown 3×10^{-11} m/W [44], bismuth (Bi) nanorods have shown 0.53×10^{-10} m/W [45] and cadmium sulfide (CdS) quantum dots have exhibited 1.9×10^{-9} m/W [46]. Similarly, many π-conjugated polymers have shown good two-photon absorption coefficients [47] on the order of 10^{-10} m/W with comparable optical limiting behavior. Recently, triphenylamine-based conjugated polymers have shown a good two-photon absorption coefficient of 1.1×10^{-10} m/W [48,10]. These values demonstrate that the present samples exhibit an optical nonlinearity comparable to those of good optical limiters reported in the literature, and are therefore potentially suitable for applications in optical limiting devices.

An increase in the planarity and rigidity of a polymer chain is known to enhance thirdorder susceptibilities because the increased rigidity optimizes the overlap of π-orbitals, which results in enhanced electron delocalization. Also, the third-order optical nonlinearity can be enhanced by an increase in the π-delocalized electron density and the carrier transport [49]. In the present

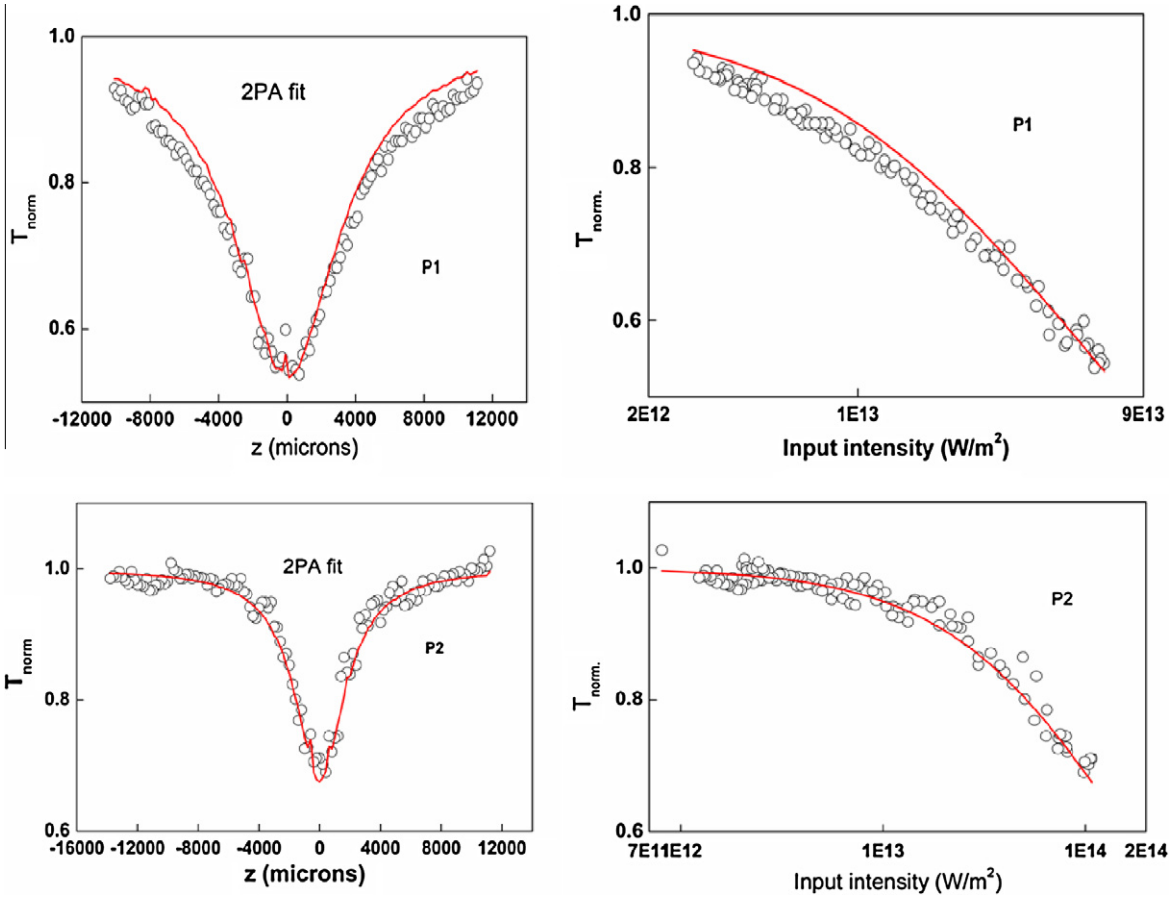

Fig. 9. Z-scan and fluence curves of **P1** and **P2.**

study, both polymers showed good optical limiting behavior and optical nonlinearity. This nonlinearity may be attributed to the presence of extended conjugation and enhanced polarizability of the molecule due to a D–A-type-arrangement in the polymer backbone. As previously discussed, the introduction of electron-deficient cyanopyridine between a highly electron-donating moiety such as alkyl-substituted diphenylamine has enhanced the D–A nature of the resulting polymer **P2** and, in turn, increased the extent of delocalization in the polymer strands. As a result, the optical nonlinearity of **P2** has increased considerably.

4. Conclusion

Two new D–A-type conjugated polymers, **P1** and **P2**, carrying highly electron-deficient cyanopyridine/oxadiazole moieties and electron-donating alkyl-substituted diphenylamine/dialkoxythiophene systems were successfully synthesized and characterized using various techniques. Linear optical studies indicated that these polymers are excellent fluorescent materials. The results of the electrochemical measurements revealed that the band gaps of the polymers were significantly reduced by an increase in the donor strength. A third-order nonlinear optical study using the Z-scan technique showed reverse saturable absorption with good TPA coefficients. The absorptive nonlinearity observed in these polymers is of the optical-limiting type. As predicted, the new polymers displayed good NLO properties, which are mainly attributed to the greater extent of delocalization and hence the increased hyperpolarizability in the molecules. They are therefore considered to be potential candidates for photonic applications.

Acknowledgements

The authors are grateful to the NITK, Surathkal; NMR Research Centre, IISc Bangalore; and SICART-CVM, Gujarat, for providing instrumental facilities.

References

[1] A.J. Heeger, Angew. Chem. Int. Ed. 40 (2001) 2591–2611.
[2] S. Kuwabara, N. Yamamoto, M. Prabhuodeyara, V. Sharma, K. Takamizu, M. Fujiki, Y. Geerts, K. Nomura, Macromolecules 44 (2011) 3705–3711.
[3] M. Lanzi, L. Paganin, D. Caretti, L. Setti, F. Errani, React. Funct. Polym. 71 (2011) 745–775.
[4] C.S. Rhett, G.T. Andrew, M.H. Lim, S.J. Lippard, Org. Lett. 7 (2005) 3573–3575.
[5] S.R. Marder, B. Kippelen, A.K.Y. Jen, N. Peyghambarian, Nature 388 (1997) 845–851.
[6] P.N. Prasad, D.J. Williams, Introduction to Nonlinear Optical Effects in Molecules and Polymers, John Wiley Inc., New York, 1991.
[7] J. Zyss, Molecular Nonlinear Optics Materials Physics and Devices, Orlando Academic Press, 1994.
[8] F. Kajzar, K.S. Lee, A.K.Y. Jen, Adv. Polym. Sci. 161 (2003) 1–85.
[9] M. Behl, E. Hattemer, M. Brehmer, R. Zentel, Macromol. Chem. Phys. 203 (2002) 503–508.
[10] J.L. Hua, B. Li, F.S. Meng, F. Ding, S.X. Qian, H. Tian, Polymer 45 (2004) 7143–7149.
[11] J. Hao, M.J. Han, K. Guo, Y. Zhao, L. Qiu, Y. Shen, X. Meng, Mater. Lett. 62 (2008) 973–976.
[12] D. Yanmaoa, J. Luc, Q. Xuc, F. Yanc, X. Xiac, L. Wangc, L. Huc, Synth. Met. 160 (2010) 409–412.
[13] R.M.F. Batista, S.P.G. Costa, M. Belsley, M.M. Raposo, Tetrahedron 63 (2007) 9842–9849.
[14] V.P. Rao, A.K.Y. Jen, K.Y. Wong, K.J. Drost, Tetrahedron Lett. 34 (1993) 1747–1750.
[15] A. Abbotto, S. Bradamante, A. Facchetti, G.A. Pagani, J. Org. Chem. 62 (1997) 5755–5759.
[16] S. Yuquan, Z. Yuxia, L. Zao, W. Jianghong, Q. Ling, L. Shixiong, Z. Jianfeng, Z. Jiayun, J. Chem. Soc., Perkin Trans. 1 (1999) 3691–3695.

[17] C.W. Dirk, H.E. Katz, M.L. Schilling, L.A. King, Chem. Mater. 2 (1990) 700–705.
[18] S.M. Tambe, A.A. Kittur, S.R. Inamdar, G.R. Mitchell, M.Y. Kariduraganavar, Opt. Mater. 31 (2009) 817–825.
[19] W.N. Leng, Y.M. Zhou, Q.H. Xu, J.Z. Liu, J. Polym. 42 (2001) 9253–9259.
[20] T. Cassano, R. Tommasi, F. Babudri, Opt. Lett. 27 (2002) 2176–2178.
[21] D. Udayakumar, A.V. Adhikari, Synth. Met. 156 (2006) 1168–1173.
[22] D. Udayakumar, A.V. Adhikari, Opt. Mater. 29 (2007) 1710–1718.
[23] S. Michelle, Liu, J. Xuezhong, S. Liu, H. Petra, A.K.Y. Jen, Macromolecules 35 (2002) 3532–3538.
[24] W. Hongli, L. Zhen, H. Bin, J. Zuoquan, L. Yanke, W. Hui, Q. Jingui, Y. Gui, L. Yunqi, S. Yinglin, React. Funct. Polym. 66 (2006) 993–1002.
[25] T.Y. Wu, N.C. Lee, Y. Chen, Synth. Met. 139 (2003) 263–269.
[26] H. Xiao, X. Lingge, Polymer 41 (2000) 9147–9154.
[27] T.M. Swager, C.G. Gil, M.S. Wrighton, J. Phys. Chem. 99 (1995) 4886–4893.
[28] S. Qingjiang, W. Haiqiao, Y. Chunhe, L. Yongfang, J. Mater. Chem. 13 (2003) 800–806.
[29] J. Pommerehe, H. Vestweber, W. Guss, R.F. Mahrt, H. Bassler, M. Porsch, Daub, J. Adv. Mater. 7 (1995) 551–554.
[30] M. Strukelji, F. Papadimitrakooulous, T.M. Miller, L.J. Rothberg, Science 267 (1995) 1969–1972.
[31] E. Perzon, X.J. Wang, S. Admassie, O. Inganäs, M.R. Andersson, Polymer 47 (2006) 4261–4268.
[32] M. Vetrichelvan, R. Nagarajan, S. Valiyaveettil, Macromolecules 39 (2006) 8303–8310.
[33] A.D. Schlüter, Polym. Sci. A: Polym. Chem. 39 (2001) 1533–1556.
[34] V.V. Jerca, F.A. Nicolescu, A. Baran, D.F. Anghel, D.S. Vasilescu, D.M. Vuluga, React. Funct. Polym. 70 (2010) 827–835.
[35] Y.P. Huang, S.H. Tsai, D.F. Huang, T.S. Tsai, T.J. Chow, React. Funct. Polym. 67 (2007) 986–998.
[36] V.D. Gupta, V.S. Padalkar, K.R. Phatangare, V.S. Patil, P.G. Umape, N. Sekar, Dyes Pigm. 88 (2011) 378–384.
[37] Z.J. Hu, P.P. Sun, L. Li, Y.P. Tian, J.X. Yang, J.Y. Wu, H.P. Zhou, L.M. Tao, C.K. Wang, M. Li, G.H. Cheng, H.H. Tang, X.T. Tao, M.H. Jiang, Chem. Phys. 355 (2009) 91–98.
[38] N.J. Turro, Modern Molecular Photochemistry Benjamin Cummings, Publ. Co., New York, 1978. p. 48.
[39] A.M. John, A.D. Panagiotis, G.M. Vasilis, T. Lin-Ren, C. Yun, Eur. Polym. J. 45 (2009) 284–294.
[40] A.P. Davey, S.O. Elliott, W. Blau, J. Chem. Soc. Chem. Commun. (1995) 1433–1434.
[41] J.K. Tai, Y.K. Jae, J.K. Kyung, L. Changjin, B.R. Suh, Synth. Met. 69 (1995) 377–378.
[42] M. Sheik-Bahae, A.A. Said, T.H. Wei, D.J. Hagan, E.W. VanStryland, IEEE J. Quant. Electron. 26 (1990) 760–769.
[43] B. Karthikeyan, M. Anija, C.S. Suchandsandeep, N.T.M. Muhammad, RejiPhilip, Opt. Commun. 281 (2008) 2933–2937.
[44] H. Nan, C. Yu, B. Jinrui, W. Jun, J.B. Werner, Z. Jinhui, J. Phys. Chem. C. 113 (2009) 13029–13035.
[45] S. Sivaramakrishnan, V.S. Muthukumar, S.S. Sivasankara, K. Venkataramanaiah, J. Reppert, A.M. Rao, M. Anija, R. Philip, N. Kuthirummal, Appl. Phys. Lett. 91 (2007) 093104–093107.
[46] P.A. Kurian, C. Vijayan, K. Sathiyamoorthy, C.S. Suchand Sandeep, P. Reji, Nano Res. Lett. 2 (2007) 561–565.
[47] M. Samoc, A. Samoc, B.L. Davies, Synth. Met. 109 (2000) 79–83.
[48] Y. Qian, K. Meng, C.G. Lu, B. Lin, W. Huan, Y. Cui, Dyes Pigm. 80 (2009) 174–180.
[49] L.P. Yu, L.R. Dalton, Synth. Met. 29 (1989) 463–470.